

Comprehensive Transcriptional Analysis of the Oxidative Response in Yeast^{*[S]♦}

Received for publication, January 11, 2008, and in revised form, March 19, 2008. Published, JBC Papers in Press, April 17, 2008, DOI 10.1074/jbc.M800295200

María Micaela Molina-Navarro^{‡1}, Laia Castells-Roca^{‡1}, Gemma Bellí[‡], José García-Martínez[§], Julia Marín-Navarro[¶], Joaquín Moreno[¶], José E. Pérez-Ortín^{¶2}, and Enrique Herrero^{‡2,3}

From the [‡]Departament de Ciències Mèdiques Bàsiques and IRBLeida, Universitat de Lleida, Montserrat Roig 2, 25008-Lleida and the [§]Departamento de Bioquímica y Biología Molecular, Facultad de Ciencias Biológicas and [¶]Sección de Chips de DNA-Servicio Central de Ayuda a la Investigación Experimental, Universitat de València, 46100-Burjassot Valencia, Spain

The oxidative stress response in *Saccharomyces cerevisiae* has been analyzed by parallel determination of mRNA levels and transcription rates for the entire genome. A mathematical algorithm has been adapted for a dynamic situation such as the response to stress, to calculate theoretical mRNA decay rates from the experimental data. Yeast genes have been grouped into 25 clusters according to mRNA level and transcription rate kinetics, and average mRNA decay rates have been calculated for each cluster. In most of the genes, changes in one or both experimentally determined parameters occur during the stress response. 24% of the genes are transcriptionally induced without an increase in mRNA levels. The lack of parallelism between the evolution of the mRNA amount and transcription rate predicts changes in mRNA stability during stress. Genes for ribosomal proteins and rRNA processing enzymes are abundant among those whose mRNAs are predicted to destabilize. The number of genes whose mRNAs are predicted to stabilize is lower, although some protein folding or proteasomal genes are among the latter. We have confirmed the mathematical predictions for several genes pertaining to different clusters by experimentally determining mRNA decay rates using the regulatable *tetO* promoter in transcriptional expression conditions not affected by the oxidative stress. This study indicates that the oxidative stress response in yeast cells is not only conditioned by gene transcription but also by the mRNA decay dynamics and that this complex response may be particularly relevant to explain the temporary down-regulation of protein synthesis occurring during stress.

Cells react against environmental stresses through multiple responses that occur at transcriptional and post-transcriptional

levels to adapt themselves to the new conditions and counteract the possible macromolecular damage caused by the stress situation. Most systematic studies on such responses focus on changes in mRNA amounts (mRNA amount or concentration (*i.e.* amount per cell), indicated as RA) caused by the environmental stress, using the DNA array technology. In the case of *Saccharomyces cerevisiae*, transcriptome analyses have been reported for a number of stresses including oxidative, osmotic, and nutritional ones in addition to heat shock (1, 2). Levels of a particular mRNA at a given time are the result of a balance between transcription rate (TR)⁴ and decay rate (commonly expressed as a half-life, or as a first-order kinetic constant of degradation, k_D) (3). It is usually assumed that TR driven by specific transcriptional regulators plays the major role in the stress response. However, decay rate may change after the onset of an environmental stress and, in that instance, profiles of individual mRNAs may not directly reflect the corresponding TR profiles. We have developed a genomic run-on (GRO) methodology that allows quantifying TR and RA for each individual gene at a genomic scale (4). Moreover, mRNA half-lives can be obtained from TR and RA data under steady-state conditions. When applied to a nutritional shift from glucose to galactose, the GRO methodology showed that TR was the main determinant of RA, although some groups of genes were modulated at the mRNA decay level (4). More recently, we have developed a mathematical algorithm to determine mRNA half-life values from pointwise measurements of TR and RA in dynamic situations after the onset of an environmental stress when steady-state conditions cannot be assumed (3). Other groups have applied nuclear run-on approaches to culture cells. Fan *et al.* (5) determined RA and TR levels in human H1299 cells for about 1000 genes under non-stress and stress conditions, from which they inferred information on mRNA decay as well. Tennebaum *et al.* (6) developed the protocol “en masse run-on assay” in which the run-on profiling is combined with ribonomic profiling. Ribonomics is a term that defines the use of immunoprecipitated mRNP complexes to analyze the representation of individual mRNA species associated with a particular RNA-binding protein. The analyses of both kinds of data have led to the proposal that “post-transcriptional operons” (7) or “decay

* This work was supported by Grants BFU2004-03167 and CSD2007-0020 (from the Ministerio de Educación y Ciencia) and 2005SGR-00677 (from the Generalitat de Catalunya) (to E.H.) and BFU2006-15446-CO3-02 and BFU2007-67575-CO3-01/BMC (from the Ministerio de Educación y Ciencia) (to J. E. P.-O.). The costs of publication of this article were defrayed in part by the payment of page charges. This article must therefore be hereby marked “advertisement” in accordance with 18 U.S.C. Section 1734 solely to indicate this fact.

♦ This article was selected as a Paper of the Week.

[S] The on-line version of this article (available at <http://www.jbc.org>) contains seven supplemental tables.

¹ Both authors contributed equally to the paper.

² Both authors contributed equally to the senior authorship of this work.

³ To whom correspondence should be addressed. Tel.: 34-973-702409; Fax: 34-973-702426; E-mail: enric.herrero@cmb.udl.cat.

⁴ The abbreviations used are: TR, transcription rate; pol I, RNA polymerase I; pol II, RNA polymerase II; GRO, genomic run-on; UTR, untranslated region; t-BOOH, *tert*-butyl hydroperoxide; RP, ribosomal proteins; GO, Gene Ontology.

regulons" (8) work in the control of eukaryotic gene expression. Decay of eukaryotic mRNA molecules may occur through different pathways (9–14). Two general mechanisms operate in *S. cerevisiae*: deadenylation of the 3'-poly(A) tail followed by 3'-5' degradation of the mRNA by the exonucleolytic activity of the exosome or initial removal of the poly(A) tail followed by mRNA hydrolysis by the 5'-3'-exonuclease Xrn1.

S. cerevisiae is the first eukaryotic organism in which whole-genome studies have been done on mRNA stability in steady-state exponential growth conditions during glucose fermentation. In a first study (8), a temperature-sensitive RNA polymerase II (pol II) mutant was employed to switch off transcription and follow up mRNA levels at successive times for each transcript. In a second study (15), several chemical inhibitors of transcription were employed for the same purpose. Both studies showed that mRNA half-lives varied between a few minutes and more than 1 h and that mRNAs for proteins involved in ribosome biogenesis and rRNA processing were relatively unstable. A general correlation was also found between mRNA decay rates and the physiological function of the gene products (8). However, the experimental conditions employed for switching off transcription in the above studies caused a stress situation *per se* in yeast cells, which discards using a similar approach for analyzing mRNA kinetics after an experimentally induced stress (16).

Oxidative stress by external agents causes a transcriptional response in *S. cerevisiae* that involves a large number of genes (1), with the participation of the general stress response factor Msn2/4p and the oxidative stress-specific transcription factors Yap1 and Skn7 (17). Exposure of yeast cells to hydrogen peroxide results in increased levels of antioxidant proteins, heat shock proteins, components of the protein degradation machinery, and enzymes of the pentose phosphate pathway, which provides NADPH for some of the antioxidant systems (18, 19). In parallel, there is a down-regulation of the protein translation apparatus. This proteome pattern, although limited to about 20% of all expressed proteins in yeast cells, approximately parallels the transcriptome pattern (1), which indicates that the oxidative stress response mainly occurs through regulation of mRNA level. However, recent studies demonstrate that inhibition of protein synthesis occurring after an oxidative stress is not only caused by transcriptional down-regulation of the translation machinery but also by inhibition of translation initiation due to dissociation of ribosomes from mRNA and a slower rate of ribosomal runoff along mRNA molecules (20, 21). This illustrates the importance of the post-transcriptional level of regulation (22), which may also involve the regulation of mRNA translation efficiency by 3'-AU-rich elements, as is the case of the *MFA2* mRNA in *S. cerevisiae* (23). The oxidative stress response in the fission yeast *Schizosaccharomyces pombe* is in part regulated by the stabilization of *atf1*⁺ mRNA mediated by the RNA-binding protein Csx1 and Upf1 (24, 25). The latter is a component of the nonsense codon-mediated mRNA decay system. Atf1 is a transcription factor that coordinates the expression of many stress response genes and itself is under regulation of the Sty1 mitogen-activated protein kinase pathway (26).

The above studies in yeast cells leave unanswered the specific role of TR and mRNA decay in establishing new mRNA levels as

a response to an oxidative stress. Here, we employ the GRO methodology to measure changes in TR and RA at a whole-genome level at different times after imposing an oxidative stress on yeast cells, and then we infer the evolution of mRNA half-lives after such a stress. Messenger RNA decay rates are validated for some genes whose expression becomes driven by the doxycycline-regulated *tet* promoter (27, 28), in conditions that do not cause an additional stress to yeast cells. Results indicate that for some functional groups of genes, changes in mRNA decay rates play an important role in the adaptation to oxidative stress.

EXPERIMENTAL PROCEDURES

Strains and Growth Conditions—Wild type *S. cerevisiae* W303-1A (*MATa ura3-1 ade2-1 leu2-3,112 trp-11 his3-11,15*) was employed in the GRO experiments. MML830 is a derivative of the above strain by integration of EcoRV-linearized pCM244 (27). This plasmid codes for the tetR'-Ssn6 protein, which acts as repressor on *tetO* promoters after activation by doxycycline. The promoter-substitution cassette from plasmid pCM224 was employed for replacing the endogenous promoters of several genes in MML830 by the *tetO*₂ promoter, as described in Ref. 28. The resulting strains are: MML863 (*tetO*₂-*HSP104*), MML957 (*tetO*₂-*RRP40*), MML980 (*tetO*₂-*HSP42*), and MML990 (*tetO*₂-*FIT3*). In these strains, the gene expression driven by *tetO*₂ is up-regulated in the absence of doxycycline, whereas the addition of the antibiotic represses it (27).

Cells were grown in YPD medium (1% yeast extract, 2% peptone, 2% glucose) at 28 °C. Doxycycline at 5 µg/ml was added for repressing genes under the *tetO*₂ promoter. Oxidative stress conditions were created by the addition of *t*-butyl hydroperoxide (*t*-BOOH) at 0.1 mM. Experiments were initiated on exponential cultures that had been grown in such conditions for at least 10 generations, at concentrations of 1.5–2 × 10⁷ cells/ml.

Genomic Run-on—Exponential cultures in 800 ml of YPD medium in 2-liter flasks shaken at 120 rpm were employed. Cell samples were taken at different times: *t*₀ (exponential growth in YPD medium, just before *t*-BOOH addition), *t*₁, *t*₂, *t*₃, *t*₄, and *t*₅, corresponding to 7, 16, 26, 41, and 71 min, respectively, after the application of the oxidative stress. At every sampling time, two different aliquots were taken. One of them was immediately processed to measure TR, according to the GRO protocol (see below). Cells from the second aliquot were recovered, washed with cold distilled water, frozen in liquid nitrogen, and stored at -80 °C until used for mRNA measurement.

The GRO protocol described previously (4) was used with the following modifications. Around 6 × 10⁸ yeast cells were used to perform *in vivo* transcription. After spinning down cells, they were washed in cold water, and the cell pellet was resuspended in 900 µl of sterile cold water (final volume 950 µl). Then, the cell suspension was transferred to a fresh microcentrifuge tube, 50 µl of 10% *N*-lauryl sarcosine sodium sulfate (sarkosyl) were added, and cells were incubated for 20 min on ice. After the permeabilization step, cells were recovered by low speed centrifugation, and the supernatant was removed. *In vivo* transcription was performed by resuspending cells in 120 µl of 2.5× transcription buffer (50 mM Tris-HCl, pH 7.7, 500 mM KCl, 80 mM MgCl₂), 16 µl of AGC mix (10 mM each of CTP,

mRNA Synthesis and Decay during the Yeast Oxidative Response

ATP, and GTP), 6 μl of dithiothreitol (0.1 M), and 13 μl of [α - ^{33}P]UTP (3000 Ci/mmol, 10 $\mu\text{Ci}/\mu\text{l}$). Cells were maintained on ice at all times. The final volume was adjusted to 300 μl with distilled water, and the mix was incubated for 5 min at 30 $^{\circ}\text{C}$ to allow transcription elongation. The reaction was stopped by adding 1 ml of cold distilled water to the mix. Cells were recovered by centrifugation to remove the non-incorporated radioactive nucleotide.

Total RNA was isolated using the Fast-Prep device (Bio101 Inc.) as described (4) except that acid phenol-chloroform (5:1) was used during cell breakage. Total extracted RNA was spectrophotometrically quantified. An aliquot was used for specific radioactivity determination in a scintillation counter. All the *in vivo* labeled RNA was used for hybridization.

Nylon filters made using PCR-amplified whole open reading frame sequences as probes (29) were used as described (4) except that hybridizations were conducted during 40–48 h. Filters were exposed for 5–7 days to an imaging plate (BAS-MP, FujiFilm), which was read in a phosphorimaging scanner (FLA-3000, FujiFilm).

Measurement of RNA Levels—As mentioned above, a second cell aliquot was taken at each sampling time and immediately frozen with liquid nitrogen. After thawing the samples on ice, total RNA was isolated following the same procedure described for GRO samples except that RNA was precipitated once with 1 volume of 5 M LiCl, washed with 70% ethanol, resuspended in distilled water, and reprecipitated with 0.1 volume of 3 M NaAcO and 2 volumes of cold 96% ethanol. Again, RNA yield was measured spectrophotometrically. About 30–40 μg of DNA-digested total RNA were reverse-transcribed into cDNA as described (4) but using Invitrogen random hexamers for random priming. Hybridization was done in the same conditions as described for the GRO experiment except that labeled cDNA was at 5×10^6 dpm/ml and that filters were exposed for 1–2 days to an imaging plate.

Estimation of Total RNA and mRNA—To facilitate further normalizations, we estimated the RNA amount obtained from a fixed amount of cells along the experiment. Thus, five different cell aliquots were taken at each of the six sampling times (t_0 – t_5) from a mock experiment. Total RNA was extracted, using the same protocol described previously, and quantified. Poly(A) mRNA was estimated using a dot-blot procedure as described (4). Using these data, we calculated the proportion of poly(A) mRNA per μg of total RNA and, thus, per cell at each of the time points (t_0 – t_5 , see Fig. 1).

Quantification of Hybridization Signals and Normalization Procedures—A total of six different nylon filters (one for each sampling time) were used. Filter combinations for the different hybridizations and replicates and image quantification were performed as described in Ref. 4. cDNA hybridizations were normalized within each experiment replicate by the global mean procedure. Correction factor to normalize between experiments was calculated from global mean values for the t_0 sampling times. Reproducibility of the replicates was tested by the ArrayStat software (Imaging Research, Inc.), considering the data as independent and allowing the program to take a minimum number of valid replicates of 2 to calculate the mean values for every gene (only one of the three replicates is allowed

to be a removable outlier). Average cDNA values for each gene were finally corrected by the percentage of guanine residues in each probe-coding strand. Normalization between sampling points was made using the amount of mRNA/cell to give values of mRNA copies/cell for each gene in every time point. These values were used for cluster analysis and comparisons.

For normalizing the GRO hybridizations a different strategy was followed. First, we measured the total transcription per cell by using total dpm measured after extraction of the *in vivo* radioactively labeled RNA. The quantification of the extracted RNA allowed us to estimate the total transcription per cell. For each time point, we estimated TR_I (TR of pol I) by summing up the 16 signals from the specific probes (eight for 18 S and eight for 25 S regions) and TR_{II} (TR of pol II) by summing up the whole set of signals (5950 pol II probes) in every hybridization. Since it is known that at t_0 (exponential growth in YPD), the ratio between TR_I and TR_{II} is about 2 (30) and that the estimated total transcription is, roughly, the sum of the contribution of these two polymerases, it is possible to determine the correction factor that fulfills these conditions. This factor was applied to the polymerase raw ratios for every sampling point. This allowed us to normalize the raw hybridization signals obtained for the RNA pol II probes. Statistical validation of replicates was performed as in cDNA values. After that, average TR values for each gene were finally corrected by the percentage of uracil residues present in each probe-coding strand. Again, the corrected average values were used for gene cluster analysis and other calculations.

Northern Blot Studies—RNA electrophoresis, probe labeling with digoxigenin, hybridization, and signal detection were done as described previously (27). Signals were quantified using the Lumi-Imager equipment (Roche Applied Science) software. Background values were determined for a region lacking visible signal, of the same size as the measured band and adjacent to it, and such background was subtracted for the respective band signal value.

k_D Calculations and Gene Classification According to Their Deviation from Constant Stability—RAs were assumed to be at a steady state at the onset of stress. Therefore, the initial (steady-state) k_D was calculated as the ratio of TR to RA values determined at time 0. After the onset of stress, under (presumably) non-steady-state conditions, the decay rates were inferred from the experimental values of TR and RA supplied by the GRO technique along the time course. Assuming a linear variation of TR in between experimentally determined values, the following relation between TR, RA, and k_D has been demonstrated to hold (3)

$$\left[\frac{(\text{TR}_2 - \text{TR}_1)}{(t_2 - t_1)} \right] - \text{TR}_2 \cdot k_D + \text{RA}_2 \cdot k_D^2 = \left[\frac{(\text{TR}_2 - \text{TR}_1)}{(t_2 - t_1)} \right] - \text{TR}_1 \cdot k_D + \text{RA}_1 \cdot k_D^2 \cdot \exp \left[-k_D \cdot (t_2 - t_1) \right] \quad (\text{Eq. 1})$$

where TR_1 , TR_2 , and RA_1 , and RA_2 are the experimentally determined values for TR and RA at successive time points t_1 and t_2 . By numerically solving for k_D (using a bisection algorithm written as a Visual Basic for Applications (VBA) program into a Microsoft Excel spreadsheet) in the above equation, a mean k_D value for the time interval between t_1 and t_2 was obtained. The absolute values of the deviations of the k_D for

every gene from its initial steady-state value (t_0) were summed up for all time points, and the sums for 4961 genes (those with values for six time points) were ranked.

Clustering Procedures—Changes in TR and RA, as well as mRNA stability estimates for all yeast genes, were evaluated by cluster analysis of normalized averaged values. For cluster analysis of the results, we used the Gene Expression Pattern Analysis Suite v 3.1 (GEPAS) included in the web server of CIPF Bioinformatic Unit, as described (4).

To test the potential enrichment in Gene Ontology (GO) categories in the different groupings obtained in this study, we used the FuncAssociate server, which uses a Monte Carlo simulation approach and accepts only significant GO categories according to their adjusted p value (computed from the fraction of 1000 simulations under the null-hypothesis with the same or smaller p value and after correction for multiple simultaneous tests). Only GO categories with an adjusted p value below 0.05 were considered to be significant.

Accession Numbers—Gene Expression Omnibus (GEO) accession numbers for the whole experiment are GSE9645 (RA data) and GSE9663 (TR data).

RESULTS

General Cell Responses to Oxidative Stress—At certain non-lethal concentrations, hydroperoxides and other oxidants cause temporary growth arrest at the G_1 stage of the *S. cerevisiae* cell cycle (31, 32). To avoid growth arrest, which could mask the direct effects of oxidative stress on general transcription and mRNA stability, we first tested a range of t -BOOH concentrations. We looked for conditions that did not affect exponential growth (when compared with control untreated cultures) but still induced expression of three reporter genes (*TRR1*, *TRX2*, *HSP12*), which have been shown to be induced by oxidative stress in previous studies (1, 33). We observed that 0.1 mM t -BOOH was the highest concentration of this oxidant that fulfilled such requirements. Therefore, all subsequent experiments were carried out with t -BOOH at 0.1 mM.

We then studied the general transcriptional responses of the cell after an oxidative stress. The total amount of poly(A) mRNA per cell decreased smoothly in the course of the experiment, whereas, as expected, cells continued proliferating (Fig. 1). Whole pol II transcription initially increased relative to time 0, an effect also observed after carbon source shift (4), to decrease at later times to levels similar to time 0. Relative TR levels did not decrease as much as relative RA levels, a fact that suggests a general mRNA destabilization following a moderate oxidative stress.

Effect of Oxidative Stress on mRNA Levels and Transcription Rates, Gene Profile Clustering—We have used the GRO experimental procedures (4) to determine the TR and RA during the *S. cerevisiae* cell response to oxidative stress. Thus, both the TR and the RA have been obtained for every yeast gene. Because we normalized the signals obtained for both parameters using a genomic DNA hybridization, values for individual genes are fully comparable. To differentiate the behaviors of the yeast genes during the stress response, we made a clustering analysis using both TR and RA data (Fig. 2). Employing the two data series allows improving gene classification because of the use of

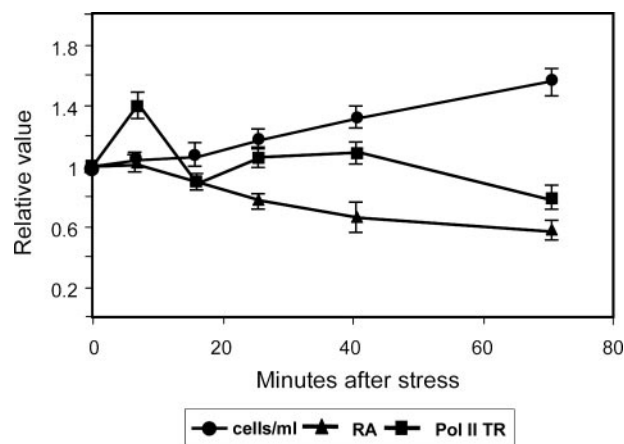


FIGURE 1. Time course of the oxidative stress experiment. At time 0, exponentially growing cells were treated with 0.1 mM t -BOOH. At the indicated times, aliquots were taken to measure cell concentration, total mRNA per cell (RA), and pol II TR per cell (see "Experimental Procedures" for details). The three parameters were referred to the respective time 0 values. Bars: standard deviation ($n = 3$).

more experimental data points. Because the raw values, or even the absolute values (supplemental Table S1), are quite different in scale for those two data sets, we used relative values to t_0 . Because of this, time points 0 for TR and RA have a 0 value in the log scale. The 12-point profiles obtained reflect the variation of TR (first six points: 0–5) and its consequence on the RA (last six points: 0–5, Fig. 2). It should be kept in mind that in our experiment, most mRNAs are probably not under steady-state conditions and that their profiles depend on TR and on mRNA stability according to kinetic laws (3).

Supplemental Table S2 lists the genes included in each cluster. In Fig. 2, the *upper main branch* of the tree (clusters 1–7) that includes 2789 genes (59%) corresponds to the genes that show a decrease in their TR along the time course. In most cases, it is followed by a decrease in RA. They correspond to repressed categories, mostly related with macromolecule biosynthesis (translation, ribosome biogenesis, transcription). The *lower main branch* of the tree (clusters 8–25) shows a transitory increase in TR that is mirrored by a transitory increase in RA in some cases (clusters 13–25, 821 genes, 17%) but not in others (clusters 8–12, 1147 genes, 24%). Clusters 13–25 correspond to genes in which RA is increased by oxidative stress (GO categories: response to stress or stimulus, ion transport, catabolism). These clusters show some differences in the timing of both peaks. In many cases, the TR peak precedes the RA one (clusters 13–19 and 22–25), but in two instances (clusters 20–21), the mRNA peaks before the TR. It is striking that clusters 8–12, however, do not show a peak in RA profile despite their TR peak. This suggests that a significant mRNA destabilization compensates (cluster 8) or even outbalances (clusters 9–12) the transcription increase. These clusters are enriched in GO categories for amino acid biosynthetic processes, oxidoreductase activity, carboxylic acid metabolism, and mitochondria. Some of these categories were analyzed further (see below).

Effect of Oxidative Stress on mRNA Stability—The first-order degradation constants (k_D , a measure of mRNA instability) can be estimated from the absolute values of TR and RA obtained by normalization of the GRO data. In a different study, we

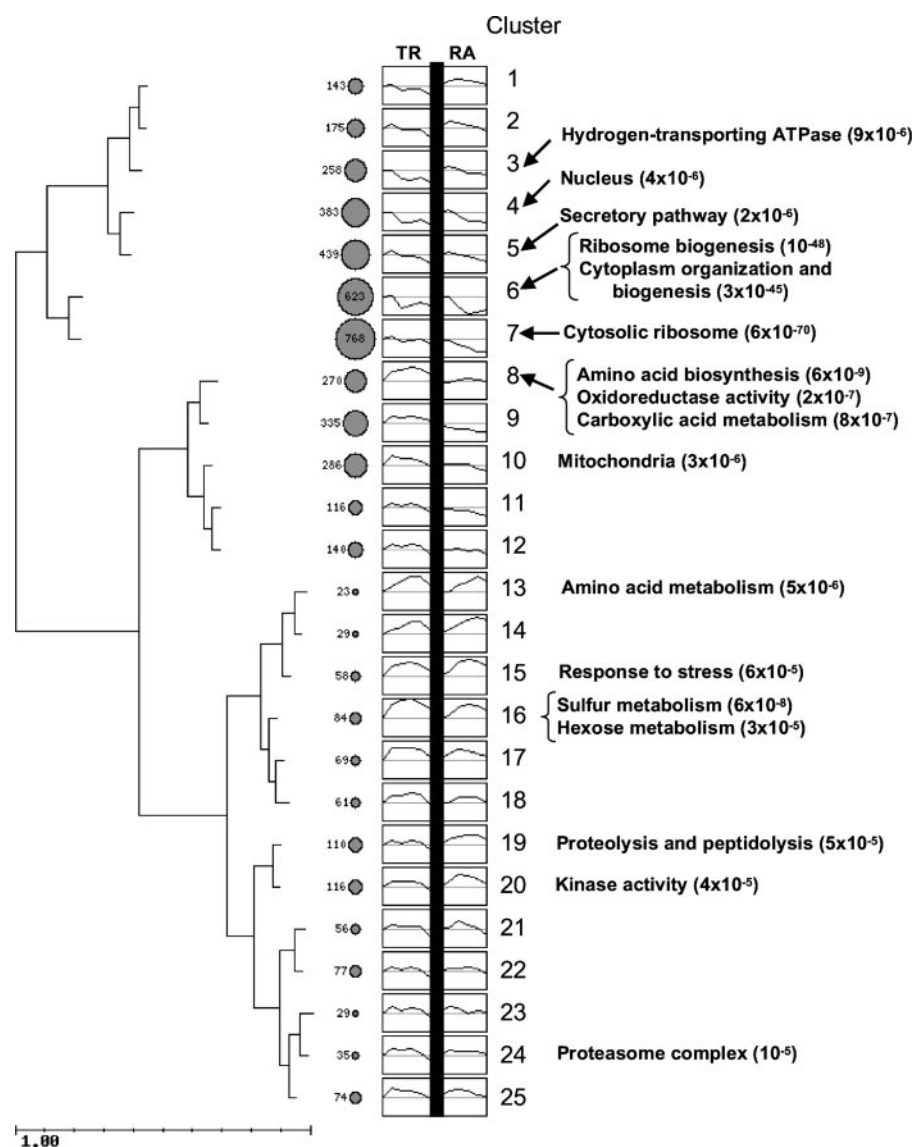


FIGURE 2. **Clustering of TR and RA data.** Time course (0, 1, 2, 3, 4, 5) profiles of both parameters were considered for clustering. Both data set series are given relative to time 0 to allow comparison between TR and RA data. The discontinuation between the last TR point and the time 0 RA value has no real meaning and, therefore, is represented as a vertical black bar. For each cluster in the tree, the number of genes contained and the data profiles are indicated. Ordinates are in log scale. The horizontal line in each graph marks the zero level. Only the most significant GO categories (p value $\leq 5 \times 10^{-5}$) are shown. Individual data for each gene can be seen in supplemental Tables S1 and S2. The scale bar in the lower left side reflects the distances between the cluster profiles.

assumed steady-state conditions for most mRNAs and determined k_D by division of RA by TR (4). However, in the current experiment, steady-state conditions are not expected to hold, at least during the first minutes of stress. Therefore, we employ here a mathematical approach based on the integration of the kinetic equations between two consecutive time points assuming a linear behavior of TR during the interval (3). Because k_D is computed from absolute values of TR and RA, which have to be calculated by comparison with external data sets, the associated error might be enlarged by the mathematical manipulation. Therefore, the k_D values obtained for individual genes (supplemental Table S1) are probably too noisy to allow further investigation. However, our analysis showed that functionally related genes follow similar behaviors in TR+RA profiles.

Therefore, we used average profiles of gene groups to describe with more confidence the kinetic behavior of mRNA stability. The average data for each one of the 25 clusters are shown in Fig. 3A. Most clusters show an initial alteration of their k_D , but they tend to return to original values. Clusters 1–12, despite their differences, show a final k_D higher than the initial one. Clusters 13–25 return to almost identical value to their initial k_D , with a slight trend to destabilization. Some clusters with barely detectable differences in TR+RA profiles show clearly distinct k_D profiles (e.g. 9 versus 10, 23 versus 24), and some clusters with quite different TR+RA profiles (e.g. 7 versus 8) show very similar k_D profiles, indicating that changes in mRNA stability are not easily deduced from RA+TR profiles during a dynamic situation. Profiles for clusters 1–5 but also for 14–17, 19, 20, and 23–25 show an initial decrease in k_D followed by a fast recovery. The particular k_D profiles are, however, different. For all these genes, it seems that stress causes a sudden mRNA stabilization whether being transcriptionally activated or not. The consequence of that stabilization is that RA increases more in the cases of up-regulation or decreases less for genes that are down-regulated. In clusters 6–12, the k_D profile shows an opposite behavior with a sudden (clusters 6–9, 11, 12) or delayed (cluster 10) mRNA destabilization. It seems, therefore, that a main contribution to RA decrease in genes related to protein biosynthesis (mostly contained in clusters 6–7) is due to mRNA destabilization. Strikingly, some genes that showed a TR increase (clusters 8–11), including the ones for amino acid biosynthesis and those related to mitochondrial function, compensate or even down-regulate their RA by means of a hyperdestabilization of their mRNAs. Finally, only a small part of yeast genes (211, with no significant enrichment in specific GO categories) have approximately flat k_D profiles (clusters 12 and 22), indicating that regulation of the mRNA stability is a general feature (>95%) of the oxidative stress response. The significance of k_D as a regulatory mechanism is better seen when yeast genes are classified according to the magnitude of k_D deviation from the steady-state value (Fig. 3B and supplemental Table S3). Some GO categories appear significantly enriched within the most affected

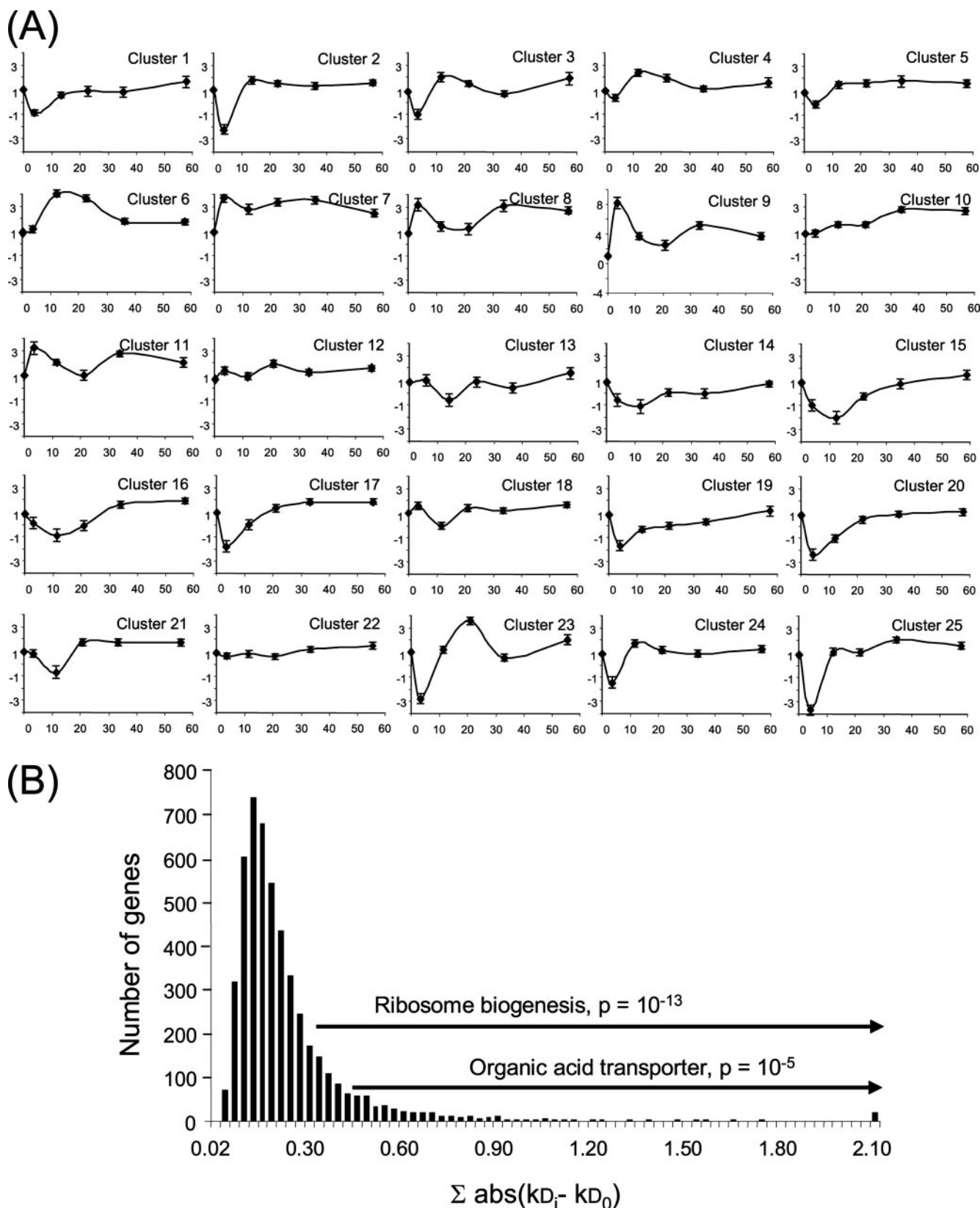


FIGURE 3. **Predicted stability of mRNAs corresponding to the different gene clusters, after an oxidative stress.** *A*, k_D values are represented in the y axis as a function of time (min) in the x axis (t -BOOH added at time 0). The graphics represent the mean k_D value corresponding to all the genes in the corresponding cluster in relative units referred to the mean k_D value at time 0. *Bars* represent the standard error for each time point. k_D scale is the same for all clusters, except for cluster 9. *B*, histogram ranking total deviations from the initial k_D during stress. The sum of differences (in absolute values) between the calculated k_D and the initial steady-state k_D (i.e. the k_D at time 0) for all time points were calculated for the whole set of individual genes. The sum values were distributed in ranges, and the number of genes in each range interval is represented. Several GO categories related to ribosome biogenesis appear as statistically significant (p value is shown) when genes with $\Sigma > 0.3$ are considered. In addition, the GO category "Organic Acid Transport" appears as significant when $\Sigma > 0.48$ is considered. Individual data can be seen in supplemental Table S3.

mRNA Synthesis and Decay during the Yeast Oxidative Response

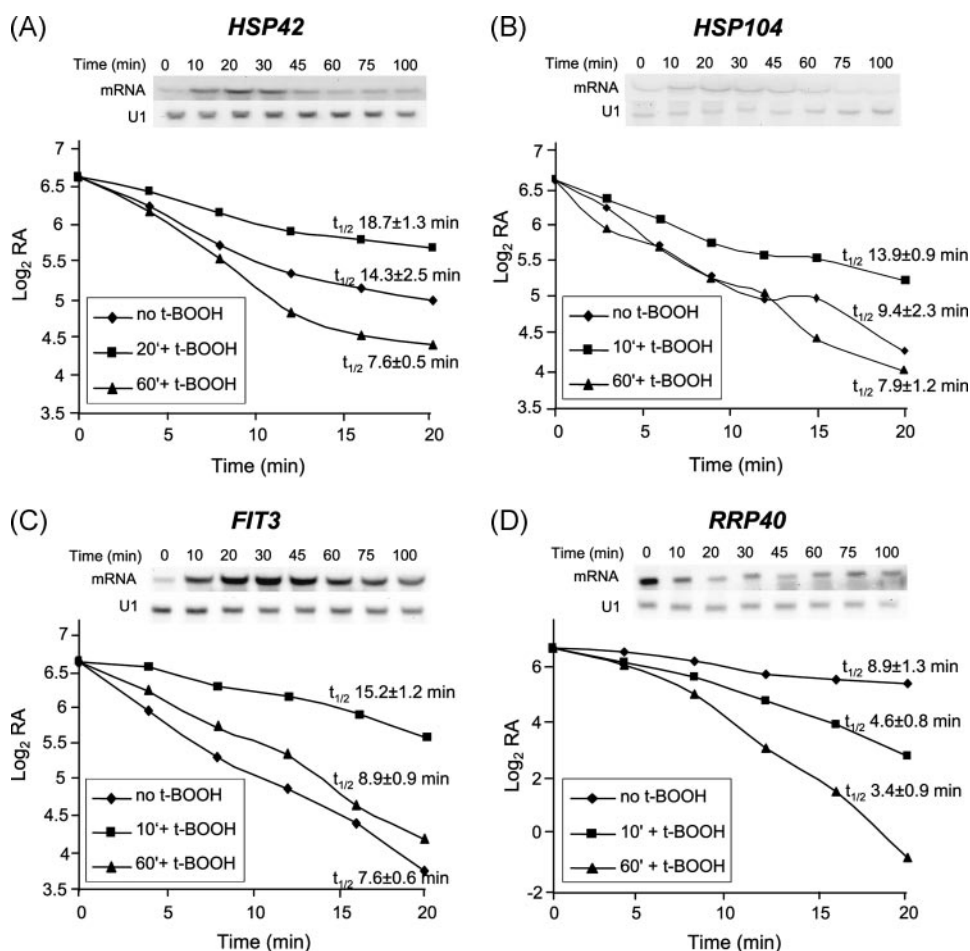


FIGURE 4. Experimental determination of mRNA half-lives before and after the addition of t-BOOH. Strains expressed *HSP42* (A, strain MML980), *HSP104* (B, MML863), *RRP40* (C, MML957), or *FIT3* (D, MML990) under the control of the *tetO₂* promoter. Doxycycline (5 μ g/ml) was added at time 0 to exponentially growing cultures of the corresponding strains at 28 °C that had not been exposed to t-BOOH or 10, 20, or 60 min after the addition of t-BOOH. In each case, aliquots were taken at time 0 and at successive times after the addition of doxycycline, for total mRNA isolation and determination of levels of the corresponding mRNA by Northern analysis. Graphics represent the evolution of experimentally determined relative RA in log scale as a function of time for a representative experiment. Mean half-life values ($t_{1/2}$) plus standard deviation for a total of three independent experiments are also indicated. To determine $t_{1/2}$ values, linear regression of experimental data (as represented in the figure) was calculated, exclusively considering only the initial points for which linearity was maintained. The upper panels show Northern analyses of RA expressed under the respective own promoters in wild type (W303-1A) cells growing exponentially after adding t-BOOH at time 0. U1 RNA is included as loading control.

by changes in stability. Genes belonging to ribosome biogenesis categories and organic acid transport are specially controlled by changes in their mRNA stability. This is the first time that such a detailed analysis of mRNA stability has been done for a dynamic situation in any organism.

Several clusters display statistically significant negative values for k_D at certain time points (particularly during the first stages of the experiment). Negative k_D values (which make obviously no biological sense) are indicative of a final excess of RA over what could be expected from a linear evolution of TR between the values experimentally determined at the beginning and the end of the time interval. We are not aware of any artifact (such as a methodological bias or a release of mRNAs from a previously undetected pool) that could cause an eventual increase of RA consistently affecting only certain clusters at definite time points. Therefore, we believe that a possible explanation of the negative k_D values is that TR did not evolve lin-

early during that time interval but followed instead a pronouncedly convex trajectory, peaking between the experimentally determined values. Indeed, it has been argued that a transient TR peak is a fit transcriptional strategy for a fast transition to a new mRNA level after an environmental shift (3). Consequently, the analysis of the k_D profiles suggests an (experimentally undetected) transient TR peak between 0 and 7 min or/and between 7 and 16 min for some clusters (Fig. 3A). This hypothesis will be investigated in the future.

Experimental Determination of mRNA Decay Rate for Some Representative Genes—We employed an experimental approach to confirm the kinetics of mRNA decay for some genes after application of an oxidative stress. For this purpose, promoters of the corresponding genes were substituted by the doxycycline-regulatable *tetO₂* promoter, and mRNA decay rates were determined in the resulting strains by measuring mRNA signal levels in Northern blots at different times after the addition of doxycycline (see “Experimental Procedures”). Previously, we had shown that down-regulation of *tet* promoters using the activator (tTA)-repressor (tetR-Ssn6) dual system occurs very shortly after the addition of doxycycline (27). For each experiment, mRNA decay rate was determined just before the addition of t-BOOH and at two different times after the

addition of the oxidant, which were selected based on the kinetics of decay according the k_D values predicted by the mathematical algorithm for each particular gene (supplemental Table S1).

Heat shock genes *HSP42* and *HSP104* are in clusters 15 and 16 respectively (supplemental Table S2). In both cases, transcript level and TR, as determined in the GRO experiment, increase transiently after the addition of the oxidant and decrease to near original values at later times (supplemental Table S1). Increase of TR precedes that of mRNA, and it is mathematically predicted for clusters 15 and 16 that mRNA molecules are transiently stabilized (lower k_D) at initial times after the onset of stress (Fig. 3A). Differences between genes in clusters 15 and 16 basically rely upon the fact that TR is more intensely up-regulated in the case of cluster 16 (Fig. 2). We confirmed by Northern analyses that *HSP42* mRNA level peaked around min 20 after the addition of the oxidant (Fig. 4A) following kinetics similar to that in the GRO experiment. The

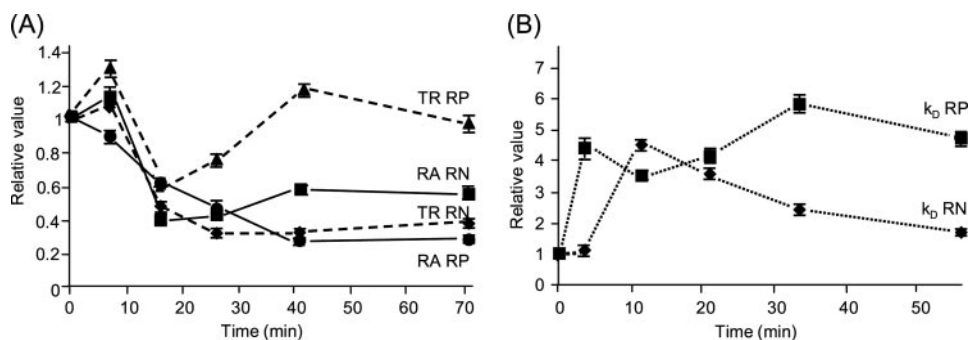


FIGURE 5. TR and RA (A) and k_D values (B) of ribosomal protein (RP) and rRNA-processing (abbreviated as RN in this figure) genes during oxidative stress. Genes in the GO categories "Ribosomal Protein" (supplemental Table S4) and "rRNA Processing" (supplemental Table S5) were considered for analysis independently of the clusters in which they were included. Mean values for the three parameters and the two categories were calculated and plotted as a function of time after *t*-BOOH addition. Represented values are relative to mean values at time 0. Bars represent the standard error for each time point.

half-life of the *HSP42* mRNA was determined before the stress and at min 20 and 60 after it (Fig. 4A). As expected (34), initial mRNA decay rates followed first-order kinetics, and half-lives were calculated from the slopes of the log curves. From a half-life value of 14.3 min during exponential growth, this increased to 18.6 min after 20 min of applying the stress, to decrease to 7.6 min after 60 min in stress conditions (Fig. 4A). That is, *HSP42* mRNA became initially stabilized, and it was destabilized at later times relative to unstressed cells. Both the initial stabilization and the final destabilization confirmed the mathematical predictions (Fig. 3A, cluster 16). A similar picture was experimentally determined for *HSP104* mRNA. Thus, there was a temporary up-regulation of mRNA levels as determined by Northern analysis and an initial transitory increase of mRNA half-life (Fig. 4B). In this case, final decay rate 60 min after the stress was close to that of unstressed cells.

Members of clusters 19 and 20 experience a much higher and rapid increase in mRNA levels than in TR upon the oxidative stress (Fig. 2), which consequently predicts a temporary stabilization of mRNAs (Fig. 3A). We tested this prediction for *FIT3*, a member of cluster 20 that shows an intense transitory up-regulation of mRNA levels in response to peroxide (Fig. 4C). The *FIT3* product is a cell wall mannoprotein that binds siderophore-iron chelates, therefore facilitating iron uptake (35). *FIT3* mRNA half-life almost doubled 10 min after the stress relative to unstressed cells, whereas at 60 min, the mRNA half-life value had approximately returned to the situation in untreated cells (Fig. 4C). This confirmed that initial stabilization of *FIT3* mRNA contributed to the transitory up-regulation of mRNA levels.

The mathematical model employed in this work predicts a temporary destabilization of mRNAs of genes in cluster 6 (Fig. 3A), which includes many genes for ribosomal proteins (RP) and for rRNA-processing proteins (supplemental Table S2). We tested this prediction for *RRP40* mRNA, whose levels and TR decrease after the onset of stress as determined by GRO, in parallel to a predicted transitory destabilization of mRNA molecules (supplemental Table S1). Northern analyses confirmed the down-regulation of *RRP40* mRNA levels upon oxidative stress (Fig. 4D). Decay kinetics showed that *RRP40* mRNA dramatically destabilized after imposing the stress, from an initial

half-life value of 8.7 min in unstressed cells to 4.7 and 3.4 min after 10 and 60 min of *t*-BOOH addition, respectively (Fig. 4D). Thus, the experimental work using the regulatable *tet* promoter system confirmed the prediction of a stress-induced mRNA destabilization.

Correlation between Transcription Parameters and Gene Function—mRNA level profiles in response to environmental stresses tend to correlate among functionally related genes (36, 37). Thus, levels of mRNA for RP and for rRNA-processing proteins decrease upon oxidative stress (1). We extended

these previous analyses to the other two mRNA-related parameters (TR, decay rate) from the GRO kinetic data (supplemental Table S1) in the oxidative stress response. 122 RP genes (most of them at cluster 7 in Fig. 2) for which time course data existed from at least two independent experiments were selected. Fig. 5 shows the global results for the whole group of genes (mean values), and supplemental Table S4 lists the results for the individual genes. Levels of mRNAs decrease steadily during the first 40 min of stress, maintaining afterward a constant value at less than 30% relative to non-stressed conditions, whereas TR decreased transitorily between 20 and 30 min to then recover afterward to control levels (Fig. 5A). This correlates with the predicted sustained destabilization of mRNAs (Fig. 5B). Similar general profiles were obtained for 135 genes in the "rRNA Processing" GO category (mainly in cluster 6 in Fig. 2), listed in supplemental Table S5. However, TR for rRNA-processing genes did not recover along the experimental period (Fig. 5A). mRNAs for this GO category were predicted to destabilize upon the stress, although at sustained lower levels than for RP mRNAs (Fig. 5B). The predicted destabilization correlates with the above results for *RRP40* mRNA (Fig. 4C). Interestingly, a modest initial up-regulation of TR was observed after oxidant addition for both RP and rRNA-processing genes (Fig. 5A).

The environmental stress response causes up-regulation of the mRNAs for proteasome subunits (1, 37). In the particular case of the oxidative stress response, it has also been shown that many proteasome subunit proteins are induced (18). We analyzed the profiles of 14 genes included in the GO category "Proteasome Core Complex" (Fig. 6 and supplemental Table S6). They are distributed among eight different clusters in Fig. 2, clusters 12 and 24 containing three genes each. In general, TR for proteasome core complex genes displayed a rapid and transitory induction to decrease below initial levels at later times (Fig. 6). This increase preceded that of mRNA levels. TR for most mRNAs coding for the proteasome core complex is coordinately up-regulated immediately after the onset of the oxidative stress, and this is followed by late repression. This by itself can explain the delayed parallel changes in mRNA levels. The coordinated behavior of TR for core proteasome genes can be related to the role of the Rpn4 transcription factor as regulator of expression of most proteasome yeast genes (38). However,

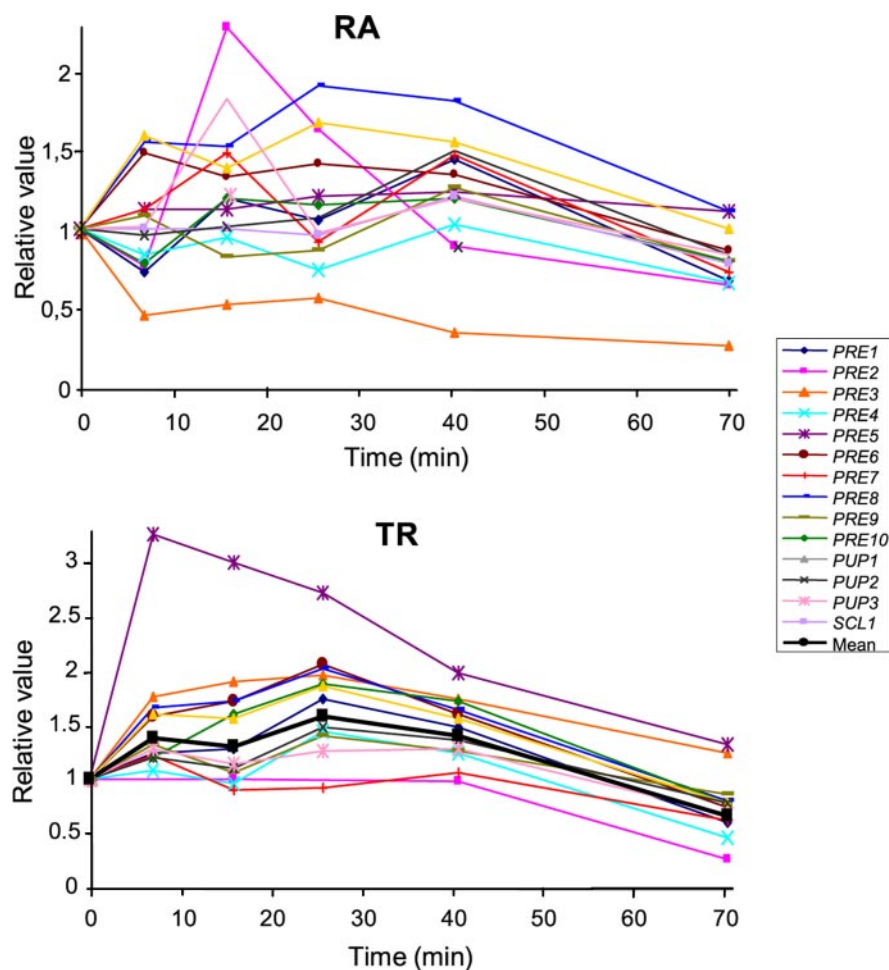


FIGURE 6. RA (upper panel) and TR value (lower panel) for genes in the GO category "Core Proteasome" as a function of time after application of an oxidative stress by *t*-BOOH. The respective genes are indicated at the right panel, and values are listed in supplemental Table S6. Represented values are relative to mean values at time 0.

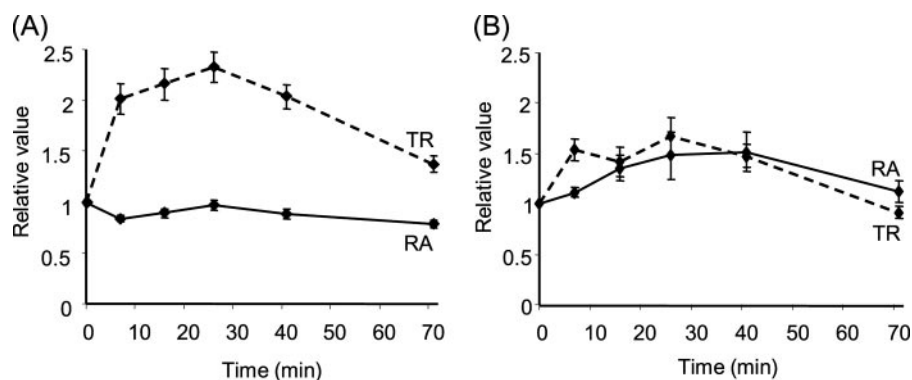


FIGURE 7. Mean TR and RA values for genes in the "Oxidoreductase Activity" GO category included in clusters 8–12 (A) or 1–7 and 13–25 (B), during oxidative stress. Represented values are relative to the unit value at time 0. Bars represent the standard error for each time point.

the RA profiles are much more variable, indicating that post-transcriptional mechanisms operate differentially on them. Analysis of genes in the GO category "Proteasome Regulatory Complex" resulted in similar patterns to those of the core complex (data not shown).

The GO category "Oxidoreductase Activity" is significantly overrepresented in cluster 8 (Fig. 2), and a number of additional

members of the category are in clusters 9–12 (supplemental Table S7). As indicated above, clusters 8–12 show an increase in TR not accompanied by RA increase. To further analyze this category, we divided oxidoreductase activity genes into those in clusters 8–12 and those in the rest of clusters (supplemental Table S7). When mean values of TR and RA are represented separately for both subgroups (Fig. 7), two different behaviors can be observed: those genes that expectedly show a parallelism between TR and RA, with a modest increase in TR preceding that of RA (clusters 1–7 and 13–25), and those that show a higher increase in TR while keeping RA basically constant, which predicts a destabilization of mRNAs (clusters 8–12). Promoter and 3'-untranslated region sequence *in silico* analysis did not evidence statistically significant enrichment of specific sequences in any of both groups of genes. Nevertheless, it is remarkable that up to one-third of oxidoreductase genes in clusters 8–12 (which would have not been detected in genomic studies strictly based on RA analyses) contain Yap1-recognizable sequences in their promoters and about 40% contain STRE sequences recognized by the Msn2/Msn4 factors. The presence of such sequences explains the TR increase upon the stress application.

DISCUSSION

In this work, we have extended previous studies on the effect of oxidative stress on mRNA amounts at the whole transcriptome level (1, 2). Thus, we have carried TR analyses and consequently predicted effects of the stress on mRNA stability. Conditions were employed in which growth was not affected after the addition of the oxidant, thereby discarding transcriptome-level effects caused by growth rate changes. Globally, pol II-mediated transcription rate did not change significantly during the examined time interval, except for a brief up-regulation at the onset of stress. However, specific sets of genes displayed higher TR values, whereas others had their TR diminished in the oxidative conditions employed.

In most of the 4757 genes (about 80% of the yeast genome) for which complete TR and RA data were obtained in this study, changes in one or both parameters occurred during the oxidative stress response. It is interesting to note that our method detects changes in gene transcription due to oxidative stress that could not be detected by conventional analyses. Thus, 1147 genes belonging to clusters 8–12 do not show an increase in RA, the usual parameter evaluated by most DNA chip analyses, but they did show an increase in TR. This means that they suffer a general destabilization in their mRNA along the time course, as shown in Fig. 3A. Therefore, we have extended the group of transcriptionally induced genes by oxidative stress by more than 2-fold: 1968 genes showing TR increase *versus* 821 that only show increase in RA. Because changes in TR are the primary consequence of the action of transcription factors, we propose that the analyses of TR changes by the GRO methodology will improve the searches (*e.g.* Ref. 39) for genes belonging to the same regulon. On the other hand, 768 genes in cluster 7 (including most RP genes, Fig. 5A) that show a significant RA down-regulation over the time course only show a minute and fluctuating TR change. Both examples illustrate the influence of mRNA stability in gene regulation and the power of our approach to detect it. Certainly, for a significant number of genes, changes occurred at modest levels. This is the case for cluster 5 (439 genes), which is characterized by a modest down-regulation (less than 50% decrease when compared with time 0) of TR and RA and is enriched in genes involved in protein secretion. Clusters 11, 12, 22, 23, and 24 also display rather constant values of TR and RA, without being enriched in particular functional categories. In total, less than one-fourth of the yeast genome maintain rather stable values (less than 2-fold changes) of both TR and RA at the oxidative stress conditions applied in this study. Clusters 6 and 7 (1391 genes) exhibit a large decrease of RA accompanied by TR down-regulation, which is more dramatic in the genes of cluster 6. The two clusters include most of the genes implicated in ribosome structure and biogenesis (RP and rRNA-processing enzymes), and this reflects the inhibition of protein synthesis after application of oxidative stress (21). However, TR inhibition alone is not sufficient to explain the decrease in RA in clusters 6 and 7 genes. The mathematical model employed here predicts a significant destabilization of mRNA molecules upon stress, which would be co-responsible for such decrease. When genes for RP and for rRNA-processing enzymes are analyzed separately from other genes in the clusters to which they pertain, an even more dramatic increase in mRNA decay rate is predicted for both groups, and we have experimentally confirmed it for *RRP40*. In ribosome-related genes, mRNA destabilization is maintained for at least 60 min after the stress. We may conclude that the down-regulation in the expression of ribosome-related genes and the subsequent inhibition of protein synthesis after an oxidative stress result from additive contributions of inhibition of transcription and increased decay rate of the respective mRNAs.

Most of the clusters from 8 to 25 display an immediate induction of TR upon the oxidative stress. For some of them, RA increase is delayed a few minutes relative to TR, as would be expected whether changes in RA were a direct consequence of TR changes (3). However, there is the exception of clusters

8–12, already commented. Clusters 13, 15, and 16 are representative of those showing an approximate parallelism between TR and RA up-regulation. These three clusters are respectively enriched in amino acid metabolism, trehalose synthesis, and sulfur metabolism genes. Activation of trehalose synthesis as a protective mechanism in response to different environmental stresses, including oxidative stress, has already been described (1). Induction of a number of pathways of amino acid biosynthesis as a response to the moderate stress conditions employed here may be an adaptive strategy to prepare cells for protein synthesis recovery. Particularly relevant is the strong induction of the biosynthetic pathway for sulfur amino acids observed in this study. Such induction has not been reported in other studies on oxidative stress responses where a higher oxidant concentration was employed (1). However, induction of this pathway by cadmium (40) and arsenite (41) has been described using genomic and proteomic approaches. Up-regulation of the sulfur amino acid pathway would thus result in higher levels of glutathione (which requires cysteine for its synthesis) needed for the redox response against oxidant conditions. Glutathione is the substrate for glutaredoxins, a group of thiol oxidoreductases participating in the oxidative stress response (42, 43). These, together with other oxidoreductases and additional enzymes detoxifying reactive oxygen species, were induced in our study. They are distributed among different clusters, especially in clusters 8 and 9.

Even for the genes (or groups of genes) with the parallel kinetics of transitory up-regulation of TR and RA, changes in mRNA decay rate may influence the response pattern. The k_D values calculated with the new algorithm may be meaningful except for cases of very fast and transitory TR responses (usually restricted to the first minutes of stress) for which the assumed linear evolution of TR in between experimental points does not hold, producing artifactual negative values of k_D . Nevertheless, negative k_D values may help to identify genes that respond to stress through short-lived abrupt TR peaks, which may be studied in the future by means of a more frequent sampling. In any case, the k_D profiles calculated by the new procedure clearly show that changes in stability are characteristic of most of the mRNAs after the oxidative stress and that the main part of their change is transitory, restricted to the first 20 min. We have studied in detail some interesting examples, such as core proteasome genes, whose mRNA levels decay at late times more slowly than TR, suggesting that mRNA stabilization is part of the stress recovery response. It is also the case for a number of genes in the "Protein Folding" GO category (data not shown in detail). We have confirmed this prediction for two heat shock proteins in this category, *HSP42* and *HSP104*. In both cases, temporary stabilization may contribute to the fact that up-regulation of RA lasts longer than that of TR. We have tested the mathematical results for a total of four examples of genes corresponding to different clusters, including the mentioned *HSP42* and *HSP104* genes, and all of them qualitatively coincide with predictions (Fig. 4). In clusters 15 and 16, although the predicted k_D values at short times are not valid, the stabilization of the mRNA is corroborated. For some functional categories, such as ribosome biogenesis and organic acid transporter (Fig. 3B) and ribosomal proteins (Fig. 5), the influence of

mRNA stability is especially important as already suggested (8, 15). Our study shows, for the first time, the extension of such a mechanism for a dynamic response in a cell.

The behavior of oxidoreductase-coding genes in clusters 8–12 deserves special attention since temporary increase in TR is not accompanied by significant changes in RA, predicting temporary mRNA destabilization upon oxidative stress. A similar situation occurs with amino acid biosynthetic genes, which are also overrepresented in clusters 8–12. Using *in silico* tools, we have not been able to detect specific sequences in promoter or terminator regions of genes for oxidoreductases, which could explain such differences between TR and RA. This leaves open the question on the molecular determinants of the lack of parallelism between both parameters. Concerning the significance of the futile transcription of a subpopulation of mRNAs to be immediately degraded, we can hypothesize that such genes may also respond to other different stresses during which they would require high transcript levels. Therefore, the promoter elements of each particular gene would be responsible for a common TR response upon the diverse stresses, but later modulation of RA would accommodate the response to each specific stress. Testing this hypothesis will require to extend this type of studies to other stresses.

In summary, analysis of TR upon a stress gives significantly more information than simply measuring changes in RA. Importantly, determining both parameters allows making inferences on how mRNA stability influences the oxidative stress response. In addition, by using a genetic system for ectopic regulation of expression of particular genes under stress in conditions not additionally influencing the cell physiology, we have been able to confirm that changes in mRNA decay rates are indeed part of the oxidative stress response for certain groups of genes. This raises the interest in searching for a mechanistic connection between oxidative stress and decay of mRNA molecules in *S. cerevisiae*, as occurs in fission yeast through the Csx1 and Upf1 proteins and the Atf1-mediated stress response (24, 25).

REFERENCES

- Gasch, A. P., Spellman, P. T., Kao, C. M., Carmel-Harel, O., Eisen, M. B., Storz, G., Botstein, D., and Brown, P. O. (2000) *Mol. Biol. Cell* **11**, 4241–4257
- Causton, H. C., Ren, B., Koh, S. S., Harbison, C. T., Kanin, E., Jennings, E. G., Lee, T. I., True, H. L., Lander, E. S., and Young, R. A. (2001) *Mol. Biol. Cell* **12**, 323–337
- Pérez-Ortín, J. E., Alepuz, P. M., and Moreno, J. (2007) *Trends Genet.* **23**, 260–267
- García-Martínez, J., Aranda, A., and Pérez-Ortín, J. E. (2004) *Mol. Cell* **15**, 303–313
- Fan, J., Yang, X., Wang, W., Wood, W. H., III, Becker, K. G., and Gorospe, M. (2002) *Proc. Natl. Acad. Sci. U. S. A.* **99**, 10611–10616
- Tenenbaum, S. A., Carson, C. C., Atasoy, U., and Keene, J. D. (2003) *Gene (Amst.)* **317**, 79–87
- Keene, J. D., and Tenenbaum, S. A. (2002) *Mol. Cell* **9**, 1161–1167
- Wang, Y., Liu, C. L., Storey, J. D., Tibshirami, R. J., Herschlag, D., and Brown, P. O. (2002) *Proc. Natl. Acad. Sci. U. S. A.* **99**, 5860–5865
- Wilusz, C. J., Wormington, M., and Peltz, S. W. (2001) *Nat. Rev. Mol. Cell Biol.* **2**, 237–246
- Chen, C. Y., Gherzi, R., Ong, S. E., Chan, E. L., Rajmakers, R., Pruijn, G. J., Stoecklin, G., Moroni, C., Mann, M., and Karin, M. (2001) *Cell* **107**, 451–464
- Parker, R., and Song, H. (2004) *Nat. Struct. Mol. Biol.* **11**, 121–127
- Maquat, L. E. (2004) *Nat. Rev. Mol. Cell Biol.* **5**, 89–99
- Newbury, S. F. (2006) *Biochem. Soc. Trans.* **34**, 30–34
- Simon, E., Camier, S., and Séraphin, B. (2006) *Trends Biochem. Sci.* **31**, 241–243
- Grigull, J., Mnaimneh, S., Pootoolal, J., Robinson, M. D., and Hughes, T. R. (2004) *Mol. Cell Biol.* **24**, 5534–5547
- Pérez-Ortín, J. E. (2008) *Brief. Funct. Genomics Proteomics* **6**, 282–291
- Toledano, M. B., Delaunay, A., Biteau, B., Spector, D., and Azevedo, D. (2003) in *Topics in Current Genetics* (Hohmann, S., and Mager, P. W. H., eds) Vol. 1, pp. 241–303, Springer-Verlag, Berlin
- Godon, C., Lagniel, G., Lee, J., Buhler, J.-M., Kieffer, S., Perrot, M., Boucherie, H., Toledano, M. B., and Labarre, J. (1998) *J. Biol. Chem.* **273**, 22480–22489
- Lee, J., Godon, C., Lagniel, G., Spector, D., Garín, J., Labarre, J., and Toledano, M. B. (1999) *J. Biol. Chem.* **274**, 16040–16046
- Swaminathan, S., Masek, T., Molin, C., Pospisek, M., and Sunnerhagen, P. (2006) *Mol. Biol. Cell* **17**, 1472–1482
- Shenton, D., Smirnova, J. B., Selley, J. N., Carroll, K., Hubbard, S. J., Pavitt, G. D., Ashe, M. P., and Grant, C. M. (2006) *J. Biol. Chem.* **281**, 29011–29021
- Sunnerhagen, P. (2007) *Mol. Genet. Genomics* **277**, 341–355
- Vasudevan, S., Garneau, N., Khounh, D. T., and Reltz, S. W. (2005) *Mol. Cell Biol.* **25**, 9753–9763
- Rodríguez-Gabriel, M. A., Burns, G., McDonald, W. H., Martin, V., Yates, J. R., III, Bähler, J., and Russell, P. (2003) *EMBO J.* **22**, 6256–6266
- Rodríguez-Gabriel, M. A., Watt, S., Bähler, J., and Russell, P. (2006) *Mol. Cell Biol.* **26**, 6347–6356
- Shiozaki, K., and Russell, P. (1996) *Genes Dev.* **10**, 2276–2288
- Belli, G., Garí, E., Piedrafitra, L., Aldea, M., and Herrero, E. (1998) *Nucleic Acids Res.* **26**, 942–947
- Belli, G., Garí, E., Aldea, M., and Herrero, E. (1998) *Yeast* **14**, 1127–1138
- Alberola, T. M., García-Martínez, J., Antúnez, O., Viladevall, L., Barceló, A., Ariño, J., and Pérez-Ortín, J. E. (2004) *Int. Microbiol.* **7**, 199–206
- Warner, J. R. (1999) *Trends Biochem. Sci.* **24**, 437–440
- Lee, J., Romeo, A., and Kosman, D. J. (1996) *J. Biol. Chem.* **271**, 24885–24893
- Wanke, V., Accorsi, K., Porro, D., Esposito, F., Russo, T., and Vanoni, M. (1999) *Mol. Microbiol.* **32**, 753–764
- Ocón-Garrido, E., and Grant, C. M. (2002) *Mol. Microbiol.* **43**, 993–1003
- Hargrove, J. L., Hulsey, M. G., and Beale, E. G. (1991) *BioEssays* **13**, 667–674
- Protchenko, O., Ferea, T., Rashford, J., Tiedeman, J., Brown, P. O., Botstein, D., and Phipps, C. C. (2001) *J. Biol. Chem.* **276**, 49244–49250
- Wu, L. F., Hughes, T. R., Davierwala, A. P., Robinson, M. D., Stoughton, R., and Altschuler, S. J. (2002) *Nat. Genet.* **31**, 255–265
- Gasch, A. P. (2003) in *Topics in Current Genetics* (Hohmann, S., and Mager, P. W. H., eds) Vol. 1, pp. 11–70, Springer-Verlag, Berlin
- Mannhaupt, G., Schnell, R., Karpov, V., Vetter, I., and Feldmann, H. (1999) *FEBS Lett.* **450**, 27–34
- Bussemaker, H. J., Hao, L., and Siggia, E. D. (2001) *Nat. Genet.* **27**, 167–171
- Fauchon, M., Lagniel, G., Aude, J. C., Lombardia, L., Soularue, P., Petat, C., Marguerie, G., Sentenac, A., Werner, M., and Labarre, J. (2002) *Mol. Cell* **9**, 713–723
- Thorsen, M., Lagniel, G., Kristiansson, E., Junot, C., Nerman, O., Labarre, J., and Tamás, M. J. (2007) *Physiol. Genomics* **30**, 35–43
- Toledano, M. B., Kumar, C., Le Moan, N., Spector, D., and Tacnet, F. (2007) *FEBS Lett.* **581**, 3598–3607
- Herrero, E., Ros, J., Belli, G., and Cabisco, E. (2008) *Biochim. Biophys. Acta* **10.1016/j.bbagen.2007.12.004**